

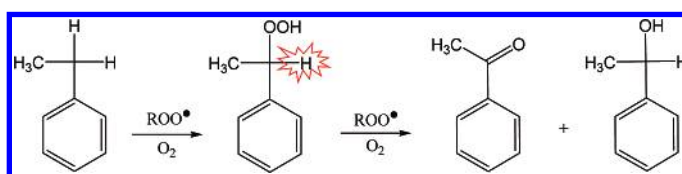
Autoxidation of Ethylbenzene: The Mechanism Elucidated

Ive Hermans,^{*,†} Jozef Peeters,[‡] and Pierre A. Jacobs[†]

Centre for Surface Chemistry and Catalysis, Department of Microbial and Molecular Systems (M²S), K.U.Leuven Kasteelpark Arenberg 23, B-3001 Heverlee, Belgium, and Division for Quantum Chemistry and Physical Chemistry, Department of Chemistry, K.U.Leuven, Celestijnenlaan 200F, B-3001 Heverlee, Belgium

ive.hermans@biw.kuleuven.be

Received January 8, 2007



Using a combined experimental and theoretical approach, we elucidated the mechanism of ethylbenzene autoxidation, at about 420 K. The generally accepted literature mechanism indeed fails to explain basic experimental observations, such as the high ketone to alcohol ratio. The hitherto overlooked propagation of 1-phenyl-ethylhydroperoxide, the primary chain product, is now unambiguously identified as the source of acetophenone as well as of 1-phenylethanol via a subsequent activated cage reaction. A similar mechanism allowed rationalizing of the cyclohexanone and cyclohexanol formation in the autoxidation of cyclohexane. The primary hydroperoxide product is found to react about 10 times faster than the arylalkane substrate with the chain carrying peroxy radicals, whereas in cyclohexane autoxidation, this reactivity ratio is as high as 55. In combination with a lower efficiency of the above-mentioned cage reaction, this results in a rather high 1-phenyl-ethylhydroperoxide yield and causes a high ketone/alcohol ratio. Radicals are shown to be predominantly generated via a concerted bimolecular reaction of the hydroperoxide with the arylalkane substrate, producing alkyl and hydrated alkoxy free radicals. In this autoxidation system, no reaction product exhibits a major initiation-enhancing autocatalytic effect, as is the case with cyclohexanone in cyclohexane autoxidation. As a result, the conversion rate increases less sharply in time compared to cyclohexane autoxidation. In fact, even some slight inhibition can be observed, due to the formation of chain-terminating HO₂[•] radicals in the alcohol co-oxidation. At 418 K, the chain length is estimated to be about 300–500 for conversions up to 10%.

Introduction

The selective oxidation of hydrocarbons by molecular oxygen is of major industrial importance, and improving its efficiency and selectivity toward the value-added products remains a prime objective.^{1–3} Important examples are the autoxidation of cyclohexane (6 × 10⁶ tons per year), yielding cyclohexanone and cyclohexanol, key intermediates in the synthesis of nylon-6 and

nylon-6,6, and the oxidation of *p*-xylene to terephthalic acid (30 × 10⁶ tons per year), a building block for poly(ethylene terephthalate). Likewise, cumene hydroperoxide (5 × 10⁶ tons per year), derived from the oxidation of cumene, serves as feedstock for both phenol and acetone. Another interesting autoxidation process is the conversion of ethylbenzene to ethylbenzene hydroperoxide (5 × 10⁶ tons per year) which is used as an epoxidizing agent in the propylene oxide/styrene process.

In view of the highly complex nature of the autoxidation mechanisms, the detailed understanding of these processes still today presents a major scientific challenge. It is widely assumed that this type of oxidation proceeds via a radical chain

* To whom correspondence should be addressed. Tel: (+32) 16 321648. Fax: (+32) 16 321998.

[†] Centre for Surface Chemistry and Catalysis, Department of Microbial and Molecular Systems (M²S).

[‡] Division for Quantum Chemistry and Physical Chemistry, Department of Chemistry.

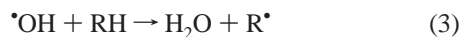
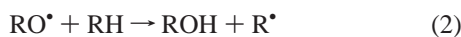
(1) Sheldon, R. A.; Kochi, J. K. In *Metal-Catalyzed Oxidations of Organic Compounds*; Academic Press: New York, 1981.

(2) Franz, G.; Sheldon, R. A. *Oxidation, Ullmann's Encyclopedia of Industrial Chemistry*; Wiley-VCH: Weinheim, 2000.

(3) Bhaduri, S.; Mukesh, D. *Homogeneous Catalysis, Mechanisms and Industrial Applications*; John Wiley & Sons: New York, 2000.

mechanism, reactions 1–6, where Q=O denotes the respective ketone formed.^{1–3}

Initiation:



Propagation:



Termination:



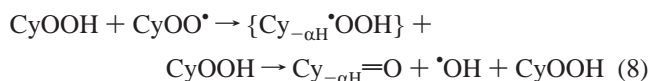
Reaction 1 represents the homolytic dissociation of the weak O–O bond in the corresponding hydroperoxide, often initially added in a small quantity to light off the reaction.¹ However, the efficiency of a unimolecular scission is very low in the liquid phase as the nascent alkoxy (RO[•]) and hydroxyl ([•]OH) radicals are prone to recombine within their solvent cage to reform ROOH faster than they can diffuse out of the Franck–Rabinowitch cage and start off new chains.⁴ Nevertheless, many autoxidation processes show a distinct autocatalytic behavior, clearly coupled to the growth of the hydroperoxide concentration. For cyclohexane (CyH), this major issue was settled by the identification of the bimolecular reaction of the hydroperoxide (CyOOH) with the ketone product (Cy_{–αH}=O) as the predominant initiation mechanism (reaction 7).⁴ In this reaction, the [•]OH radical breaking away from the hydroperoxide abstracts an αH-atom from Cy_{–αH}=O, producing the resonance-stabilized ketonyl radical (Cy_{–αH,–βH}=O or Q_{–αH}=O) and a cyclohexoxy radical (CyO[•]), hydrogen bonded to H₂O. These effects combine to reduce the energy barrier and prevent geminate recombination of the product radicals in their solvent cage, thus greatly enhancing the efficiency of this initiation mechanism.



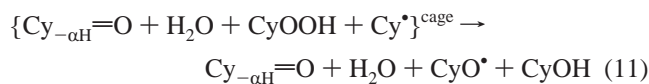
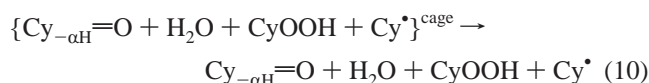
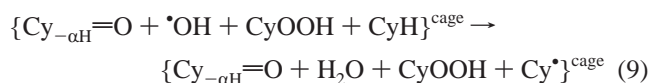
Carbon-centered radicals R[•], formed via the fast reactions 2 and 3, rapidly react with dioxygen (reaction 4), producing the chain carrying peroxy radicals (ROO[•]). These radicals can abstract H-atoms from the substrate (reaction 5), yielding ROOH and new R[•] radicals. Reactions 4 and 5 are chain-propagating reactions, which conserve the number of radicals. When the hydroperoxide product can efficiently initiate new radical chains via, e.g., reaction 7 for the CyH case, this mechanism should indeed be referred to as autocatalytic.⁴ The propagation sequence is repeated many times before the peroxy radicals are destroyed in the termination reaction (6), producing an alcohol (ROH) and a ketone (Q=O). This termination reaction balances the chain initiation reaction, leading to a fast radical quasisteady state.⁵ Under normal autoxidation conditions, the ratio of the

rates of propagation and termination, i.e., the chain length, is very large, resulting in a *radical chain* mechanism.

Recently, we demonstrated that the mechanism outlined in reactions 1–6, though widely accepted over many decades, fails utterly to explain product formation in the autoxidation of cyclohexane.^{6,7} Indeed, given the long radical chain length of about 100, the slow chain termination reaction (6), with a rate equal to the (equally slow) initiation step, can only account for a very small fraction of the observed alcohol and ketone molecules. A combination of state-of-the-art theoretical methodologies and experiments demonstrated that cyclohexyl peroxy radicals (CyOO[•]) abstract not only hydrogen atoms from the substrate molecule (CyH) but also, and much more rapidly, the weakly bonded αH-atom from CyOOH. The ratio of the propagation rate constants for both H-abstraction reactions, $k_{\text{CyOOH}}/k_{\text{CyH}}$, was determined to be as high as 55.^{6,7} The resulting α-hydroperoxy-alkyl radicals are demonstrated to be unstable and to dissociate promptly into [•]OH and Q=O (reaction 8), without any energy barrier.⁸ This CyOOH propagation is thus identified as the fast ketone source that was missing in the literature so far.



The exothermic dissociation of Cy_{–αH}•OOH into Cy_{–αH}=O and [•]OH is rapidly followed by an H-abstraction by the “hot” [•]OH radical from an ubiquitous RH molecule in the solvent cage around the nascent products,⁹ producing even more heat (reaction 9). The overall exothermicity of more than 60 kcal/mol causes the formation of a nanosized hot spot, several hundred degrees kelvin above the bulk temperature, governing the fate of the cage products.⁶ Indeed, although reaction 10, the out-of-cage diffusion, features a lower activation barrier, the subsequent activated-cage reaction (11) accounts for the majority of the reaction flux (about 70%), due to the high cage temperature. This cage reaction was identified as the missing source of CyOH and was shown at the same time to account for the observed net removal of CyOOH.^{6,7}



The CyO[•] coproduct radicals not only abstract H-atoms from the substrate (reaction 2) but also undergo ring-opening via β

(6) Hermans, I.; Nguyen, T. L.; Jacobs, P. A.; Peeters, J. *Chem. Phys. Chem.* **2005**, *6*, 637.

(7) Hermans, I.; Jacobs, P. A.; Peeters, J. *J. Mol. Catal. A: Chem.* **2006**, *251*, 221.

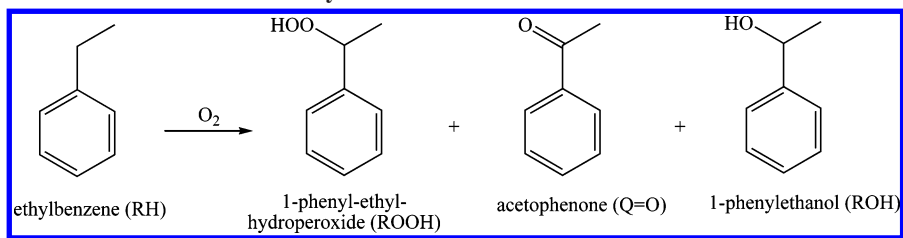
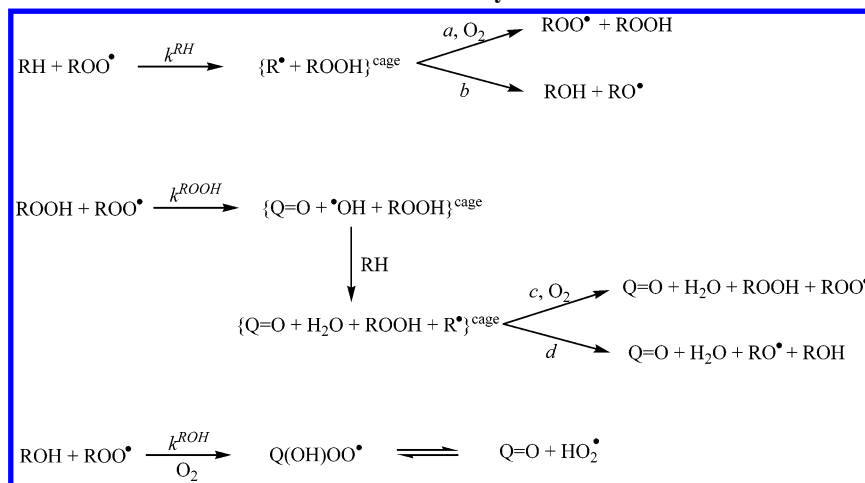
(8) Vereecken, L.; Nguyen, T. L.; Hermans, I.; Peeters, J. *Chem. Phys. Lett.* **2004**, *393*, 432.

(9) At the high temperature of the hot spot, the reactions of the nascent [•]OH radical with RH and ROOH are nearly equally fast, such that the larger number of RH molecules, making up the cage wall, as compared to the single ROOH molecule inside the cage will result in [•]OH reacting mainly with RH.

(4) Hermans, I.; Jacobs, P. A.; Peeters, J. *Chem.–Eur. J.* **2006**, *12*, 4229.

(5) The characteristic lifetime τ of ROO[•] radicals is given by $1/\{2 \times k^{\text{term}} \times [\text{ROO}^\bullet]\}$. Even at very low conversions, τ is much shorter than the timescale over which [ROO[•]] changes significantly, such that a radical quasisteady state will be established throughout the reaction.

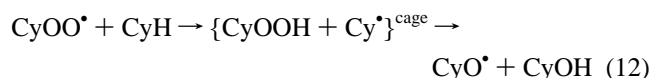
SCHEME 1. Overall Autoxidation Reaction of Ethylbenzene

SCHEME 2. Proposed Reaction Scheme for the Autoxidation of Ethylbenzene^a

^a Q stands for R- α H, in casu Ph-C-CH₃.

C–C cleavage.¹ Thus, cage reaction 11 was also found to account for the majority of the ring-opened (acidic) byproducts in the autoxidation of cyclohexane.^{7,10}

An analogous cage reaction can also occur after the H-abstraction from CyH (reaction 12). As this cage reaction is not activated, its efficiency is much smaller, so that it contributes to only 5% of the CyH propagation flux.⁶ Still, this minor reaction channel readily explains the direct formation of (some) CyOH from CyH,¹¹ which thus far could not be rationalized.



The peroxy radical can also abstract the α H-atom from CyOH. Though this reaction is slower than reaction 8, it is still important as $k^{\text{CyOH}}/k^{\text{CyH}} \approx 10$.^{6,7} The α -hydroxy-alkylperoxy radical (Cy- α H(OH)OO \bullet), formed upon addition of O₂, was shown to rapidly equilibrate with its products, Cy- α H=O and HO₂ \bullet .¹² This equilibrium is strongly shifted toward the products, thus constituting another, though minor, ketone source.⁶ More importantly, the very fast, diffusion-controlled radical-termination reaction (13) was argued to cause a substantial decrease in the peroxy radical concentration, such that the CyOH coautoxidation significantly slows the overall kinetics.



(10) Hermans, I.; Jacobs, P. A.; Peeters, J. *Chem.–Eur. J.* **2007**, *13*, 754.

(11) Berezin, I. V.; Denisov, E. T.; Emanuel, N. M. *The Oxidation of Cyclohexane*; Pergamon Press: New York, 1996.

(12) Hermans, I.; Müller, J.-F.; Nguyen, T. L.; Jacobs, P. A.; Peeters, J. *J. Phys. Chem. A* **2005**, *109*, 4303.

Cy- α H=O was found to be somewhat less reactive than CyOH toward CyOO \bullet ($k^{\text{Q=O}}/k^{\text{CyH}} \approx 5$), making Cy- α H=O only a limited source of byproducts,^{6,7,10} in contrast to earlier literature views.^{1–3} On the other hand, Cy- α H=O was shown to greatly enhance radical initiation via an efficient bimolecular initiation step (7),⁴ as discussed above.

The objective of the present work is to elucidate the detailed mechanism responsible for the autoxidation of ethylbenzene (Scheme 1), which not only is an important bulk process by itself but also can serve as a model for the oxidation scheme of arylacetic esters and heterocyclic acetic esters,¹³ relevant in fine chemical applications.

Similar to CyH autoxidation, the primary chain propagation step, ROO \bullet + RH, is expected to involve α H-abstraction from the secondary –CH₂– alkyl substituent moiety. As a working hypothesis, it is reasonable to propose an ethylbenzene oxidation mechanism (Scheme 2) along the same lines as that for CyH. The specific resonance-stabilized Q \bullet OOH radical, resulting from the α H-abstraction from 1-phenyl-ethylhydroperoxide by ROO \bullet , was earlier shown to decompose in the absence of an energy barrier into the corresponding ketone and \bullet OH.⁸

Results and Discussion

1. Experimental Observations. Figure 1a shows the ethylbenzene to product conversion in time. For safety reasons, the conversion was limited to less than 10% to avoid a build-up of peroxides. A short induction period, during which radicals need to be formed via unfavorable pathways, can be observed. Such an induction stage can be bypassed if a small amount of ROOH

(13) See, e.g.: Wentzel, B. B.; Donners, M. P. J.; Alsters, P. L.; Feiters, M. C.; Nolte, R. J. M. *Tetrahedron* **2000**, *56*, 7797.

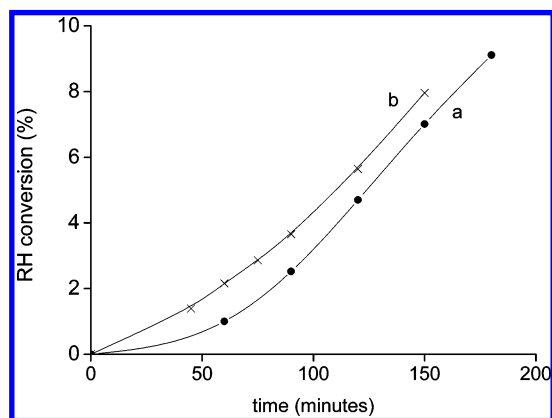


FIGURE 1. Ethylbenzene conversion in time at 418 K: (a) pure ethylbenzene, (b) ethylbenzene with 0.7 mol % of 1-phenyl-ethyl-hydroperoxide initially added.

is initially added (Figure 1b). In contrast to cyclohexane autoxidation,^{4,6} the conversion increases nearly linearly, rather than exponentially, pointing to the less-pronounced autocatalytic nature of ethylbenzene autoxidation.

Obviously, at low conversions, the overall oxidation rate, $d\Sigma[P]/dt$, is equal to the RH conversion rate by reaction 5 (eq 1).

$$d\Sigma[P]/dt = k^{\text{RH}} \times [\text{ROO}^*] \times [\text{RH}] \quad (\text{eq 1})$$

The rate constant for RH propagation, k^{RH} , can be estimated as follows. At the validated B3LYP/6-311++G(df,pd)//B3LYP/6-31G(d,p) level of theory,⁶ the barrier for H-abstraction from ethylbenzene by CH_3OO^* radicals was calculated to be 12.06 kcal/mol. Combining this activation barrier with the measured k^{RH} at 303 K, $1.3 \text{ M}^{-1} \text{ s}^{-1}$,¹⁴ allows the calculation of a pre-exponential (TST) rate factor per H-atom of $3.25 \times 10^8 \text{ M}^{-1} \text{ s}^{-1}$.¹⁵ It follows that k^{RH} is equal to $6.5 \times 10^8 \text{ M}^{-1} \text{ s}^{-1} \times \exp(-12.06 \text{ kcal mol}^{-1}/RT)$. On the basis of the experimental $d\Sigma[P]/dt$ and k^{RH} at 418 K of $320 \text{ M}^{-1} \text{ s}^{-1}$, one can estimate the 1-phenyl-ethylperoxyl radical concentration, using expression 1. Thus, with 0.7 mol % of ROOH initially added and after 1.0% RH conversion, i.e., for $[\text{ROOH}] = 0.13 \text{ M}$, one finds $[\text{ROO}^*] \approx 1.9 \times 10^{-8} \text{ M}$. Combining this number with the rate constant for chain termination, $k^{\text{term}}(418 \text{ K}) = 1.8 \times 10^8 \text{ M}^{-1} \text{ s}^{-1}$ (vide infra), a chain length of 385 is obtained. This large number demonstrates indeed that chain termination reaction 6 cannot be responsible for a sizable fraction of the reaction products as often assumed.¹ Moreover, according to the classical mechanism (reactions 1–6), the expected Q=O/ROH ratio should be close to 1/2, whereas an experimental value of approximately 2 is observed. Indeed, according to this simple scheme, ketone is produced exclusively in the termination reaction whereas an almost equal amount of additional alcohol originates from reaction 2, following the initiation step (see also below). In fact, even more alcohol could be produced via an

(14) Howard, J. A. Reactions of Organic Peroxyl Radicals in Organic Solvents. In *Peroxy Radicals, The Chemistry of Free Radicals*; Alfassi, Z. B., Ed.; John Wiley & Sons: Chichester West Sussex, 1997; p 283.

(15) This value is in good agreement with the pre-factor per H-atom, A^{perH} , derived from the known rate constant for $\text{CH}_3\text{OO}^* + \text{C}_3\text{H}_8 \rightarrow \text{CH}_3\text{-OOH} + \text{iso-C}_3\text{H}_7^*$ at 400 K, i.e., $0.96 \text{ M}^{-1} \text{ s}^{-1}$,¹⁶ and the calculated barrier of 16.1 kcal/mol, i.e., $A^{\text{perH}} = 3.0 \times 10^8 \text{ M}^{-1} \text{ s}^{-1}$.

(16) Tsang, W. J. *Phys. Chem. Ref. Data* **1988**, 17.

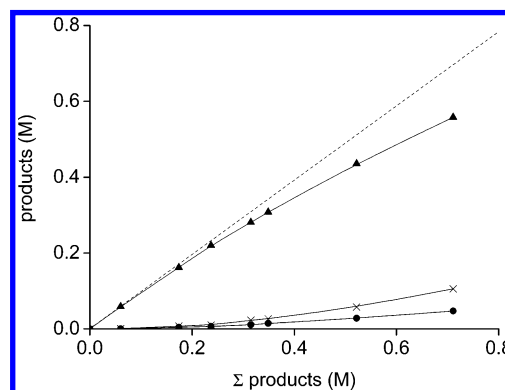


FIGURE 2. Product distribution against the sum of products in the 418 K autoxidation of ethylbenzene: 1-phenyl-ethyl-hydroperoxide (▲); acetophenone (×); and 1-phenylethanol (●).

often overlooked nonterminating peroxy self-reaction, $\text{ROO}^* + \text{ROO}^* \rightarrow \text{RO}^* + \text{RO}^* + \text{O}_2$.¹⁷

In Figure 2, the product distribution is plotted against the sum of products. Only products arising from the oxidation of secondary C–H bonds in the substrate could be observed (Scheme 1). This plot clearly identifies ROOH as the only primary reaction product, whereas both ROH and Q=O are secondary products and must therefore originate from ROOH. A striking observation is the high peroxide selectivity (e.g., 83% after 6.3% conversion), compared to the cyclohexyl hydroperoxide selectivity in the autoxidation of cyclohexane (only 25% after 6.3% conversion).⁶

2. Input from Computational Chemistry. The higher 1-phenyl-ethylhydroperoxide yield from ethylbenzene should be ascribed to a significantly reduced $k^{\text{ROOH}}/k^{\text{RH}}$ ratio compared to the $k^{\text{CyOOH}}/k^{\text{CyH}}$ ratio of 55 for cyclohexane. This ratio corresponds to the αH -abstraction reactions from the (aryl)-alkane substrate and the corresponding hydroperoxide by the dominant chain-propagating peroxy radicals, i.e., 1-phenyl-ethylperoxyl and cyclohexylperoxyl, respectively. This is rationalized in Figure 3 by comparing the calculated activation barrier for the abstraction of H-atoms from different alkanes and their corresponding hydroperoxides by the CH_3OO^* radical. It can be observed that the reactivity difference between the hydroperoxide and the alkane decreases when the substrate becomes more reactive. For substrates with secondary C–H bonds (C–H BDE₀ = 96.6 kcal/mol), the difference in the abstraction barrier between the alkane and the peroxide is predicted to be 5.5 kcal/mol, whereas for substrates featuring much weaker bonds (such as ethylbenzene, C–H BDE₀ = 80.5 kcal/mol), this difference decreases to only 1.9 kcal/mol. Therefore, it is predicted that the αH -abstraction of 1-phenyl-ethylhydroperoxide is only about 5 times as fast as the H-abstraction from the parent alkane. The barrier for abstraction of the αH -atom from 1-phenylethanol is calculated to be 2.5 kcal/mol lower than that from the RH substrate. A $k^{\text{ROH}}/k^{\text{RH}}$ ratio of about 10 seems reasonable, implying that the observed Q=O/ROH ratio of 2 cannot be ascribed to a fast subsequent oxidation of the alcohol.

(17) Lightfoot, P. D.; Cox, R. A.; Crowley, J. N.; Destriau, M.; Hayman, G. D.; Jenkin, M. E.; Moortgat, G. K.; Zabel, F. *Atmos. Environ.* **1992**, 26A, 1805.

(18) Luo, Y.-R. *Handbook of Bond Dissociation Energies in Organic Compounds*; CRC Press: Boca Raton, 2003.

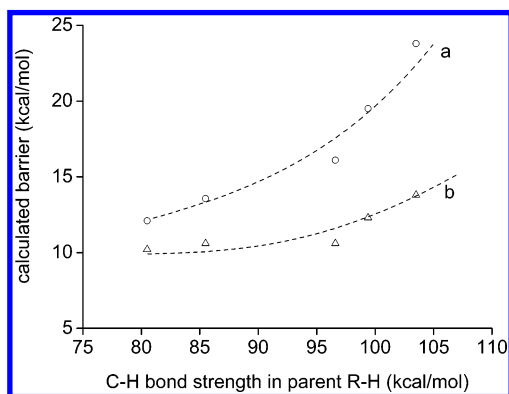
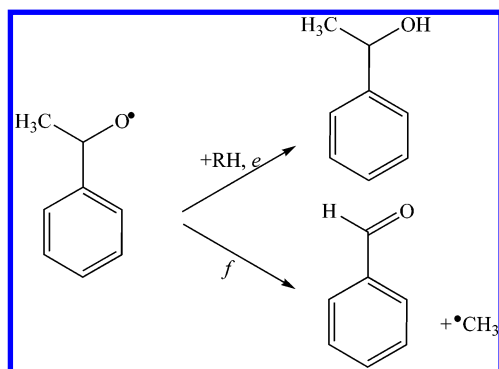


FIGURE 3. Computed barriers for the abstraction of H-atoms from different alkanes (a) and from the corresponding hydroperoxides (b) as a function of the alkane C–H bond strength,¹⁸ reduced to 0 K. Substrates from left to right: ethylbenzene, toluene, propane (H^{sec}), ethane, and methane.

SCHEME 3. Pathways for Reaction of the RO[•] Alkoxy Radical



Next, the fate of the RO[•] radicals is addressed. These alkoxy radicals can abstract H-atoms from the alkane substrate or decompose via β -scission (Scheme 3). The rate of H-abstraction (fraction e in Scheme 3) can be estimated as follows. Given the 298 K rate constant of the CyO[•] + CyH and (CH₃)₃CO[•] + CyH abstraction reactions of 8.0×10^5 and 9.2×10^5 M⁻¹ s⁻¹, respectively,^{19,20} and the calculated barrier of (CH₃)₂CHO[•] + CyH of 4.7 kcal/mol, one can estimate a pre-exponential (TST) rate factor per H^{sec}-atom of 2.0×10^8 M⁻¹ s⁻¹, in line with the analogous pre-factor per H-atom for abstractions by ROO[•] radicals (i.e., 3.25×10^8 M⁻¹ s⁻¹, vide supra). Note that the influence of the alkyl group in the oxy radical on the abstraction reaction from a given substrate is very small. Combining this pre-factor with the barrier for H-abstraction from PhCH₂CH₃ by (CH₃)₂CHO[•], a model for RO[•], i.e., 3.2 kcal/mol, shows a rate constant of 8.5×10^6 M⁻¹ s⁻¹ at 418 K. The pseudo-first-order rate constant for RO[•] removal via H-abstraction can thus be estimated at $\approx 7 \times 10^7$ s⁻¹. On the other hand, the β -cleavage of PhCH(O[•])–CH₃ (fraction f in Scheme 3) proceeds at a rate of $k(T) = 5.3 \times 10^{13} \times \exp(-12.7 \text{ kcal/mol}/RT)$ s⁻¹ (TST calculation based on a B3LYP/6-31G(d,p)-PES, known to give reliable results for this type of reaction²¹). Clearly, for this specific RO[•] radical, the H-abstraction channel will be favored: $e \approx 0.9$ and $f \approx 0.1$, as witnessed by the absence of

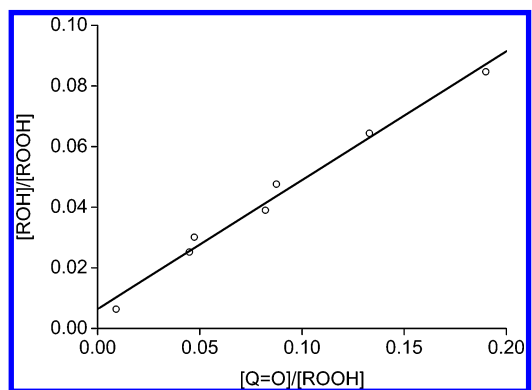


FIGURE 4. Plot of the experimental [ROH]/[ROOH] ratio vs the [Q=O]/[ROOH] ratio, validating eq 2: intercept = 0.006 ± 0.002 , slope = 0.425 ± 0.02 , correlation coefficient = 0.993.

benzaldehyde, or its oxidation product benzoic acid, in the reaction mixture.²²

3. Reaction Analysis. Following the mechanism outlined in Scheme 2, but neglecting the integrated effect of ROH coautoxidation for a conversion up to 10%, eq 2 can be derived based on a stoichiometric ROOH balance.⁷

$$\frac{[\text{ROH}]}{[\text{ROOH}]} \approx \frac{b}{a}(1 + e) + \frac{d}{a}(1 + e) \frac{[\text{Q=O}]}{[\text{ROOH}]} \quad (\text{eq 2})$$

In Figure 4, the [ROH]/[ROOH] ratio is plotted vs the [Q=O]/[ROOH] ratio, demonstrating that at up to nearly 10% conversion the linear relation proposed in eq 2 is observed indeed. From the intercept of the plot in Figure 4, and using $e \approx 0.9$, it follows that fractions a and b are equal to 0.997 and 0.003, respectively. Apparently, the cage fraction is nearly negligible, in contrast to the case of cyclohexane autoxidation where the value of b is equal to 0.05. This difference can be readily understood when comparing the computed activation energy for this cage reaction: for cyclohexane and ethylbenzene, this barrier is 6.8 vs 8.4 kcal/mol, respectively (B3LYP/6-31G(d,p) level). Obviously, the higher barrier must be attributed to resonance stabilization in the R[•] radical, lowering its reactivity. From the slope of Figure 4, values can be obtained for the fractions c and d of 0.78 and 0.22, respectively. The efficiency of the activated cage reaction is also much lower than that for cyclohexane, due to this difference in activation barriers.

As the ratio of branching ratios, $(d/c)/(b/a) \approx 95$, should equal $\exp[\Delta E/R \times \Delta(1/T)]$, with ΔE being the difference between the barrier of the activated cage reaction (≈ 8.4 kcal/mol) and the barrier for diffusive separation (≈ 1.5 kcal/mol) and $\Delta(1/T)$ referring to the difference between the hot spot T and the bulk T ($=418$ K), one can estimate an effective hot spot T of $\approx 900 \pm 200$ K. This is in line with the rough estimation stemming from the 65 kcal/mol of heat released in the fast propagation process.

Within the frame of the new reaction mechanism, eq 3 can be derived on the basis of a kinetic analysis of the alcohol and ketone formation rates.⁷

$$\frac{[\text{ROOH}]}{[\text{RH}]} \times \frac{d[\text{ROH}]}{d[\text{Q=O}]} \approx (1 + e) \times b \times \frac{k^{\text{RH}}}{k^{\text{ROOH}}} + (1 + e) \times d \times \frac{[\text{ROOH}]}{[\text{RH}]} \quad (\text{eq 3})$$

(19) Druliner, J. D.; Krusic, P. J.; Lehr, G. F.; Tolman, C. A. *J. Org. Chem.* **1985**, *50* (26), 5843.

(20) Weber, M.; Fischer, H. *J. Am. Chem. Soc.* **1999**, *121* (32), 7381.

(21) Peeters, J.; Fantechi, G.; Vereecken, L. *J. Atmos. Chem.* **2004**, *48*, 59.

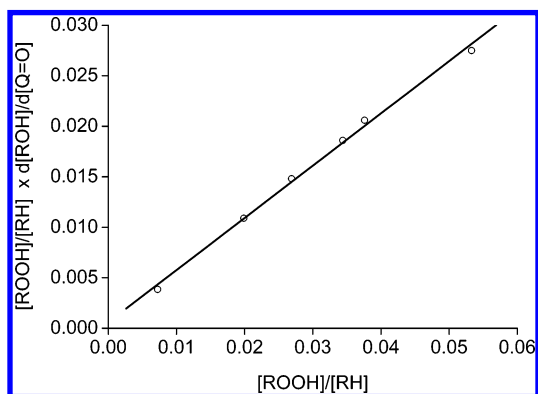


FIGURE 5. Validation of eq 4 by plotting the experimental $[\text{ROOH}]/[\text{RH}] \times d[\text{ROH}]/d[\text{Q}=\text{O}]$ product ratio vs the $[\text{ROOH}]/[\text{RH}]$ ratio: intercept = $(5.8 \pm 5.0) \times 10^{-4}$, slope = 0.52 ± 0.01 , correlation coefficient = 0.999.

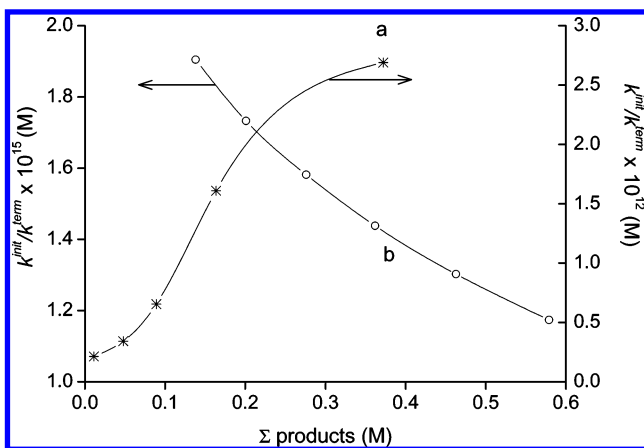


FIGURE 6. Measured $k^{\text{init}}/k^{\text{term}}$ ratio vs the sum of products during the autoxidation of cyclohexane (a) and ethylbenzene (b) at 418 K.

In Figure 5, the experimentally determined left-hand side of eq 3, corrected for ROH co-oxidation, is plotted against the $[\text{ROOH}]/[\text{RH}]$ ratio. Again, a linear relation is observed. Combining the intercept of the plot in Figure 5 with the value of b derived above, we can estimate the $k^{\text{ROOH}}/k^{\text{RH}}$ ratio at 10 ± 10 , in agreement with the first principles prediction used above. The $k^{\text{ROOH}}/k^{\text{RH}}$ ratio can also be extracted from the relative ROOH conversion, viz., $\{\Sigma[\text{P}] - [\text{ROOH}]\}/0.5 \cdot \{[\text{ROOH}](0) + [\text{ROOH}](t)\}$, where the rate-averaged $[\text{ROOH}]$ (0 to t) is approximated by $0.5\{[\text{ROOH}](0) + [\text{ROOH}](t)\}$, and the relative RH conversion, viz., $\Sigma[\text{P}]/[\text{RH}]$, taking into account that ROOH is only consumed in the activated cage reaction, viz., channel d in Scheme 2 (eq 4).

$$k^{\text{ROOH}}/k^{\text{RH}} \approx \frac{\{\Sigma[\text{P}] - [\text{ROOH}]\}/0.5 \cdot \{[\text{ROOH}](0) + [\text{ROOH}](t)\}}{\Sigma[\text{P}]/[\text{RH}]} \times \frac{1}{d} \quad (\text{eq 4})$$

The average value obtained for $k^{\text{ROOH}}/k^{\text{RH}}$ via eq 4 is equal to 20 ± 10 , in line with the analysis above. From the slope of the plot in Figure 5, a value for fraction d of 0.27 is obtained, also in good agreement with the value derived from eq 2.

The reason for the much higher peroxide yield in the ethylbenzene autoxidation than in the cyclohexane oxidation can thus be attributed to (i) the significantly lower relative

reactivity of the hydroperoxide, and (ii) the lower efficiency of the activated cage reaction which is a net sink of hydroperoxide (see Scheme 2).

4. Formation of New Radicals During the Chain Initiation.

As the $k^{\text{ROOH}}/k^{\text{RH}}$ ratio is now known, eq 1 can be corrected by taking into account the additional RH consumption, subsequent to the hydroperoxide propagation (see Scheme 2), leading to eq 5.

$$d\Sigma[\text{P}]/dt = \{(1 + b \times e) \times k^{\text{RH}} \times [\text{ROO}^*] \times [\text{RH}]\} + \{(1 + d \times e) \times k^{\text{ROOH}} \times [\text{ROO}^*] \times [\text{ROOH}]\} \quad (\text{eq 5})$$

This expression allows for a more accurate estimation of the peroxy radical concentration, which can ultimately be used to evaluate $k^{\text{init}}/k^{\text{term}}$, via the radical quasisteady state⁵ (eq 6).

$$k^{\text{term}} \times [\text{ROO}^*]^2 = k^{\text{init}} \times [\text{ROOH}] \quad (\text{eq 6})$$

Whereas $k^{\text{init}}/k^{\text{term}}$ increases by an order of magnitude during autoxidation of cyclohexane (Figure 6a), a moderate but monotone decrease of this ratio can be observed during ethylbenzene autoxidation (Figure 6b). The pronounced autocatalytic effect in the CyH autoxidation was earlier ascribed to occurrence of reaction 7: cyclohexanone is efficiently assisting the CyOOH molecules to initiate new radical chains.⁴ Due to the very fast increase in cyclohexanone during CyH autoxidation, $k^{\text{init}}/k^{\text{term}}$ also increases sharply. Nevertheless, at higher CyH conversions, the enhancement of the initiation was found to be counteracted by HO_2^* formation, as witnessed by the sigmoidal shape of the $k^{\text{init}}/k^{\text{term}}$ ratio (Figure 6a).⁴ As the αH -atoms of acetophenone are bound more strongly than those in cyclohexanone, the former compound is much less efficient in assisting the hydroperoxide cleavage. Actually, a steady decrease in $k^{\text{init}}/k^{\text{term}}$ can be observed during the ethylbenzene autoxidation. This remarkable effect was also observed by Korthals Altes et al., when examining the ethylbenzene oxidation rate, derived from the O_2 consumption, as a function of $[\text{ROOH}]^{0.5}$ (i.e., $\propto [\text{ROO}^*]$, eq 6).²³ To explain this enigmatic behavior, this early study proposed additional termination channels of $^*\text{OH}$ and RO^* radicals with each other and with the main chain propagator ROO^* as becoming important at higher conversions. However, even when taking into account the hitherto overlooked $^*\text{OH}$ and RO^* sources via the ROOH propagation (vide supra), the $^*\text{OH}$ and RO^* concentrations remain very small throughout the reaction due to their fast H-abstraction reactions with RH, i.e., $k = 2 \times 10^9$ and $8.5 \times 10^6 \text{ M}^{-1} \text{ s}^{-1}$, respectively, at 418 K. Thus, as an example, for $[\text{ROOH}] = 0.13 \text{ M}$ and $[\text{ROO}^*] = 1.9 \times 10^{-8} \text{ M}$ (vide supra), $[^*\text{OH}]$ and $[\text{RO}^*]$ are calculated to be only 3×10^{-16} and $1.3 \times 10^{-13} \text{ M}$, respectively. Therefore, even diffusion-controlled termination channels involving these radicals will remain entirely negligible compared to the ROO^* self-reaction (6).

A far more reasonable explanation for the observed decrease in the $k^{\text{init}}/k^{\text{term}}$ ratio is the formation of HO_2^* radicals in the co-oxidation of ROH.¹² Indeed, given the predicted $k^{\text{ROOH}}/k^{\text{RH}}$ ratio of 10 (vide supra) and the observed ROH/RH ratio of 0.008 at 10% conversion, the HO_2^* production can be estimated to be a fraction 0.08 of the ROO^* production. Taking into account the high cross-termination rate constant for HO_2^* radicals with

(22) Cleavage of the $\text{Ph}-\text{CH}(\text{O}^*)\text{CH}_3$ bond, yielding Ph^* and CH_3CHO , faces a barrier of 18.5 kcal/mol and can therefore be ruled out completely.

(23) Korthals Altes, F. W.; van den Berg, P. J. *Recueil* **1966**, *85*, 538.

ROO^\bullet ($\approx 2 \times 10^9 \text{ M}^{-1} \text{ s}^{-1}$)²⁴ vs the mutual termination rate constant for ROO^\bullet radicals ($1.8 \times 10^8 \text{ M}^{-1} \text{ s}^{-1}$, vide infra), this small amount of HO_2^\bullet can indeed enhance the apparent termination rate constant by a factor of about 2. This corresponds to the observed decrease in the $k^{\text{init}}/k^{\text{term}}$ ratio in Figure 6b. From the $k^{\text{init}}/k^{\text{term}}$ ratio, extrapolated to zero conversion, i.e., $2.3 \times 10^{-15} \text{ M}$, and the mutual termination rate constant for ROO^\bullet radicals, k^{init} can be evaluated. It is reasonable to adopt a termination rate constant for 1-phenyl-ethylperoxyl radicals similar to that for phenyl-methylperoxyl (=benzylperoxyl) radicals, i.e., $1.8 \times 10^8 \text{ M}^{-1} \text{ s}^{-1}$, at 418 K from recent gas-phase rate coefficient measurements^{25,26} and the known temperature dependence of the nontermination/termination branching ratio.¹⁷ Indeed, for fast self-reacting ROO^\bullet radicals such as benzylperoxyl, an additional substituent on the αC (i.e., a methyl group) appears to affect the rate constant only marginally. Using a value for k^{term} of $1.8 \times 10^8 \text{ M}^{-1} \text{ s}^{-1}$, a pseudo-first-order k^{init} of $4 \times 10^{-7} \text{ s}^{-1}$ is found; this value is in line with the apparent pseudo-first-order rate constant for the “pure” CyOOH initiation in the cyclohexane autoxidation.⁴

In our detailed studies on the initiation of cyclohexane autoxidation, we concluded that even the so-called “pure” initiation is in fact a bimolecular reaction of $\text{CyO}-\text{OH}$ with $\text{Cy}-\text{H}$, reaction 14, with a rate constant of $1.0 \times 10^{-7} \text{ M}^{-1} \text{ s}^{-1}$ at 418 K and an experimental Arrhenius activation energy of about 25 kcal/mol, which is significantly lower than the $\text{CyO}-\text{OH}$ BDE of $\approx 40 \text{ kcal/mol}$.⁴



Likewise, an experimental rate constant for reaction 15 of $5 \times 10^{-8} \text{ M}^{-1} \text{ s}^{-1}$ can be derived, which is two times smaller than that for the analogous reaction with CyH . This result should be attributed to the larger number of H^{sec} -atoms in cyclohexane compared to ethylbenzene, compensated by a lower calculated energy barrier for reaction 15, i.e., 26.6 vs 28.1 kcal/mol for reaction 14 (B3LYP/6-311++G(df,pd)//B3LYP/6-31G(d,p) level).



Figure 7 compares the potential energy surface of this bimolecular initiation mechanism (15) with the hitherto assumed homolytic cleavage, reaction 1. Clearly, the newly proposed reaction is energetically favorable and proceeds through a loose TS ($\text{O} \cdots \text{O}$ length $\approx 1.98 \text{ \AA}$). An analogous initiation reaction between two ROOH molecules can be neglected, based on the 25.1 kcal/mol energy barrier and the low ROOH/RH ratio.

Whereas the main fate of the nascent RO^\bullet and $^\bullet\text{OH}$ radicals in the case of the homolytic dissociation will be in-cage recombination, the sharp potential energy drop after the TS of the bimolecular initiation mechanism (15) forces a translational separation of the two radical fragments. Moreover, in-cage combination is also reduced by the 3.2 kcal/mol strong H-bond between H_2O and RO^\bullet , screening the radical site in the alkoxy radical. Therefore, in ethylbenzene autoxidation, radicals should predominantly be formed via reaction 15. The derived rate of

this reaction is in good agreement with its predicted energy barrier and the analogous reaction in CyH autoxidation.

The improved peroxy radical concentration, obtained via eq 5, can also be used to get a more accurate value of the chain length. Due to the nearly linear increase of the ROOH concentration as a function of $\Sigma[\text{P}]$ (Figure 2), the ROO^\bullet concentration also increases because the rate of chain initiation is proportional to $[\text{ROOH}] \times [\text{RH}]$ (vide supra). As a consequence, the chain length is found to decrease upon increasing conversion, although it remains very high (Figure 8).

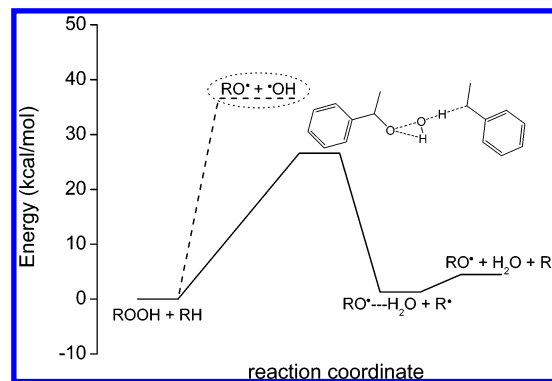


FIGURE 7. Potential energy surface of the homolytic dissociation of ROOH , compared with the bimolecular reaction (15).

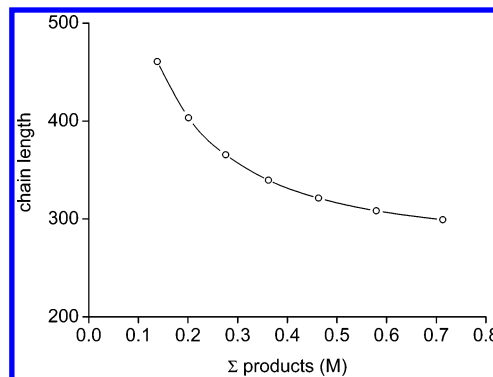


FIGURE 8. Evaluated chain length vs the sum of products during the 418 K autoxidation of ethylbenzene.

Conclusions

In this contribution, the mechanism of ethylbenzene autoxidation was studied in detail, combining complementary experimental and theoretical methodologies. The hitherto widely accepted reaction scheme was unable to explain several experimental observations pertaining to the basics of the mechanism. This literature mechanism attributed the formation of ketone exclusively to the slow termination reaction between two chain carrying peroxy radicals; this reaction, together with the initiation that should proceed at an equal rate, would result in an expected alcohol/ketone ratio of at least 2 because the nonterminating mutual peroxy reaction to form the alkoxy radicals plus oxygen must lead to additional alcohol. Experimentally, however, an alcohol/ketone ratio of 0.5 is observed over a wide conversion range. More importantly, the radical chain length of this process is so long (>300) that the termination and initiation reactions cannot possibly contribute significantly to the product flux; obviously, it is the much faster chain-propagation steps of the peroxy radicals that determine

(24) Rowley, D. M.; Lesclaux, R.; Lightfoot, P. D.; Nozière, B.; Wallington, T. J.; Hurley, M. D. *J. Phys. Chem.* **1992**, *96*, 4889.

(25) Nozière, B.; Lesclaux, R.; Hurley, M. D.; Dearth, M. A.; Wallington, T. J. *J. Phys. Chem.* **1994**, *98*, 2864.

(26) Dib, G. E.; Chakir, A.; Roth, E.; Brion, J.; Daumont, D. *J. Phys. Chem. A* **2006**, *110*, 7848.

the product makeup. Indeed, the fairly high observed yields of ketone and alcohol and the experimental alcohol/ketone ratio of 0.5 can be readily explained in the frame of a new reaction scheme. This revised mechanism attributes the formation of acetophenone to the α H-abstraction from 1-phenyl-ethylhydroperoxide by the chain-propagating 1-phenyl-ethylperoxyl radical and formation of 1-phenylethanol to a subsequent activated cage reaction, analogous to the formation of cyclohexanone and cyclohexanol in the autoxidation of cyclohexane. The ethylbenzene-derived hydroperoxide is indeed about 10 times more reactive toward the chain-propagating peroxyl radical than the arylalkane substrate itself. Interestingly, as a comparison, cyclohexylhydroperoxide reacts even about 55 times faster than its cyclohexane parent with cyclohexylperoxyl radicals. A straightforward explanation for this difference in behavior was found in the convergence of the reactivity of hydroperoxides and their parent alkanes as the alkane C–H bond becomes weaker. Additionally, it was discovered that, due to a higher activation barrier, the efficiency of the above-mentioned cage reaction is much lower than that in the cyclohexane autoxidation. The combined effects afford a higher hydroperoxide yield and a reversed ketone/alcohol ratio compared to cyclohexane autoxidation. Beside elucidating the formation mechanism of the major reaction products, also the detailed mechanism of chain initiation was identified and kinetically quantified. Radicals are shown to be predominantly generated via a concerted bimolecular reaction of the hydroperoxide with the arylalkane substrate, producing $\text{RO}\cdot\cdots\text{H}_2\text{O} + \text{R}\cdot$. In this autoxidation system, there is no reaction product with a major initiation-enhancing autocatalytic effect, as cyclohexanone has

in the cyclohexane autoxidation. As a result, the conversion rate increases less sharply in time than in cyclohexane autoxidation. In fact, an observed decrease in the $k^{\text{init}}/k^{\text{term}}$ ratio, attributed to enhanced termination by $\text{HO}_2\cdot$ radicals arising from alcohol coautoxidation, indicates a slight inhibition of the radical chain mechanism.

This study shows the generic character of the newly proposed autoxidation mechanism of (substituted) alkanes. It enables us to explain quantitatively the product distribution for two entirely different substrates in a straightforward way and is fully backed up by quantum chemical calculations. The detailed knowledge of the chemistry at issue constitutes a great leap forward in understanding the reaction and possibly in further optimization of this important process.

Experimental and Theoretical Methods

The autoxidation of ethylbenzene (50 mL, p.a.) was studied at 418 K in a 100 mL stainless steel high-pressure Parr reactor, stirred at 500 rpm. Before heating the reactor, it was pressurized with 2.76 MPa of dioxygen (99.99% purity). Prior to each experiment, the reactor was passivated with a saturated sodium pyrophosphate (p.a.) solution.⁶ The products were quantified by GC-FID, after the addition of an external standard (1-heptanol, p.a.) via a double injection: trimethyl phosphine (1 M in THF) was added to one of the samples to reduce the peroxide product to the alcohol. From the quantified alcohol content before and after reduction, both the alcohol and peroxide yields can be determined. The injection-port temperature of the GC was set at 250 °C. Peak areas were converted to concentrations by means of the specific sensitivities determined by direct calibrations.

Quantum chemical (QC) calculations were carried out with the GAUSSIAN03 program.²⁷ At the DFT level, the Becke three-parameter hybrid exchange functional was used, combined with the Lee–Yang–Parr nonlocal correlation functional B3LYP-DFT.²⁸ Unless stated otherwise, the B3LYP/6-311++G(d,p)//B3LYP/6-31G(d,p) level of theory was used, which was shown earlier to agree within 0.5 kcal/mol with state-of-the-art computational levels for H-abstractions by peroxyl radicals.⁶ For other reactions, the accuracy of the calculated barriers is estimated to be ± 2 kcal/mol.²⁹ Rate coefficients of predominant reaction steps in the mechanism were evaluated by means of transition-state theory (TST), using the QC-generated energy and ro-vibrational parameters.³⁰ For some specific reaction types, TST pre-factors validated by experimental data were adopted from the literature.

Acknowledgment. This work was performed in the framework of an IAP project (federal government), IDECAT (European government), CECAT (K.U.Leuven) and two GOA projects (K.U.Leuven). I.H. thanks the FWO for a research position.

Supporting Information Available: Geometries and energetic and vibrational data of interesting structures are provided. This material is available free of charge via the Internet at <http://pubs.acs.org>.

JO070040M

(27) Frisch, M. J.; Trucks, G. W.; Schlegel, H. B.; Scuseria, G. E.; Robb, M. A.; Cheeseman, J. R.; Montgomery, J. A., Jr.; Vreven, T.; Kudin, K. N.; Burant, J. C.; Millam, J. M.; Iyengar, S. S.; Tomasi, J.; Barone, V.; Mennucci, B.; Cossi, M.; Scalmani, G.; Rega, N.; Petersson, G. A.; Nakatsuji, H.; Hada, M.; Ehara, M.; Toyota, K.; Fukuda, R.; Hasegawa, J.; Ishida, M.; Nakajima, T.; Honda, Y.; Kitao, O.; Nakai, H.; Klene, M.; Li, X.; Knox, J. E.; Hratchian, H. P.; Cross, J. B.; Bakken, V.; Adamo, C.; Jaramillo, J.; Gomperts, R.; Stratmann, R. E.; Yazyev, O.; Austin, A. J.; Cammi, R.; Pomelli, C.; Ochterski, J. W.; Ayala, P. Y.; Morokuma, K.; Voth, G. A.; Salvador, P.; Dannenberg, J. J.; Zakrzewski, V. G.; Dapprich, S.; Daniels, A. D.; Strain, M. C.; Farkas, O.; Malick, D. K.; Rabuck, A. D.; Raghavachari, K.; Foresman, J. B.; Ortiz, J. V.; Cui, Q.; Baboul, A. G.; Clifford, S.; Cioslowski, J.; Stefanov, B. B.; Liu, G.; Liashenko, A.; Piskorz, P.; Komaromi, I.; Martin, R. L.; Fox, D. J.; Keith, T.; Al-Laham, M. A.; Peng, C. Y.; Nanayakkara, A.; Challacombe, M.; Gill, P. M. W.; Johnson, B.; Chen, W.; Wong, M. W.; Gonzalez, C.; Pople, J. A. *Gaussian 03*, revision C.02; Gaussian, Inc.: Wallingford, CT, 2004.

(28) (a) Becke, A. D. *J. Chem. Phys.* **1992**, *96*, 2115. (b) Becke, A. D. *J. Chem. Phys.* **1992**, *97*, 9173. (c) Becke, A. D. *J. Chem. Phys.* **1993**, *98*, 5648. (d) Lee, C.; Yang, W.; Parr, R. G. *Phys. Rev. B* **1988**, *37*, 785.

(29) See, e.g.: (a) Young, D. C. *Computational Chemistry*; John Wiley & Sons: New York, 2001. (b) Koch, W.; Holthausen, M. C. *A Chemist's Guide to Density Functional Theory*, 2nd ed.; Wiley-VCH: Weinheim, 2001.

(30) (a) Eyring, H. *J. Chem. Phys.* **1934**, *3*, 107. (b) Steinfeld, J. I.; Francisco, J. S.; Hase, W. L. *Chemical Kinetics and Dynamics*; Prentice Hall: New Jersey, 1989.